

1 ***Supporting Information Appendix***

2 **Higher mortality rates leave heated ecosystem with similar size-**
3 **structure despite larger, younger, and faster growing fish**

4 Max Lindmark^{a,1}, Malin Karlsson^a, Anna Gårdmark^b

5

6 ^a Swedish University of Agricultural Sciences, Department of Aquatic Resources, Institute of
7 Coastal Research, Skolgatan 6, 742 42 Öregrund, Sweden

8 ^b Swedish University of Agricultural Sciences, Department of Aquatic Resources, Box 7018,
9 750 07 Uppsala, Sweden

10

11 ¹ Author to whom correspondence should be addressed. Current address:

12 Max Lindmark, Swedish University of Agricultural Sciences, Department of Aquatic
13 Resources, Institute of Marine Research, Turistgatan 5, 453 30 Lysekil , Sweden, Tel.:
14 +46(0)104784137, email: max.lindmark@slu.se

15

16

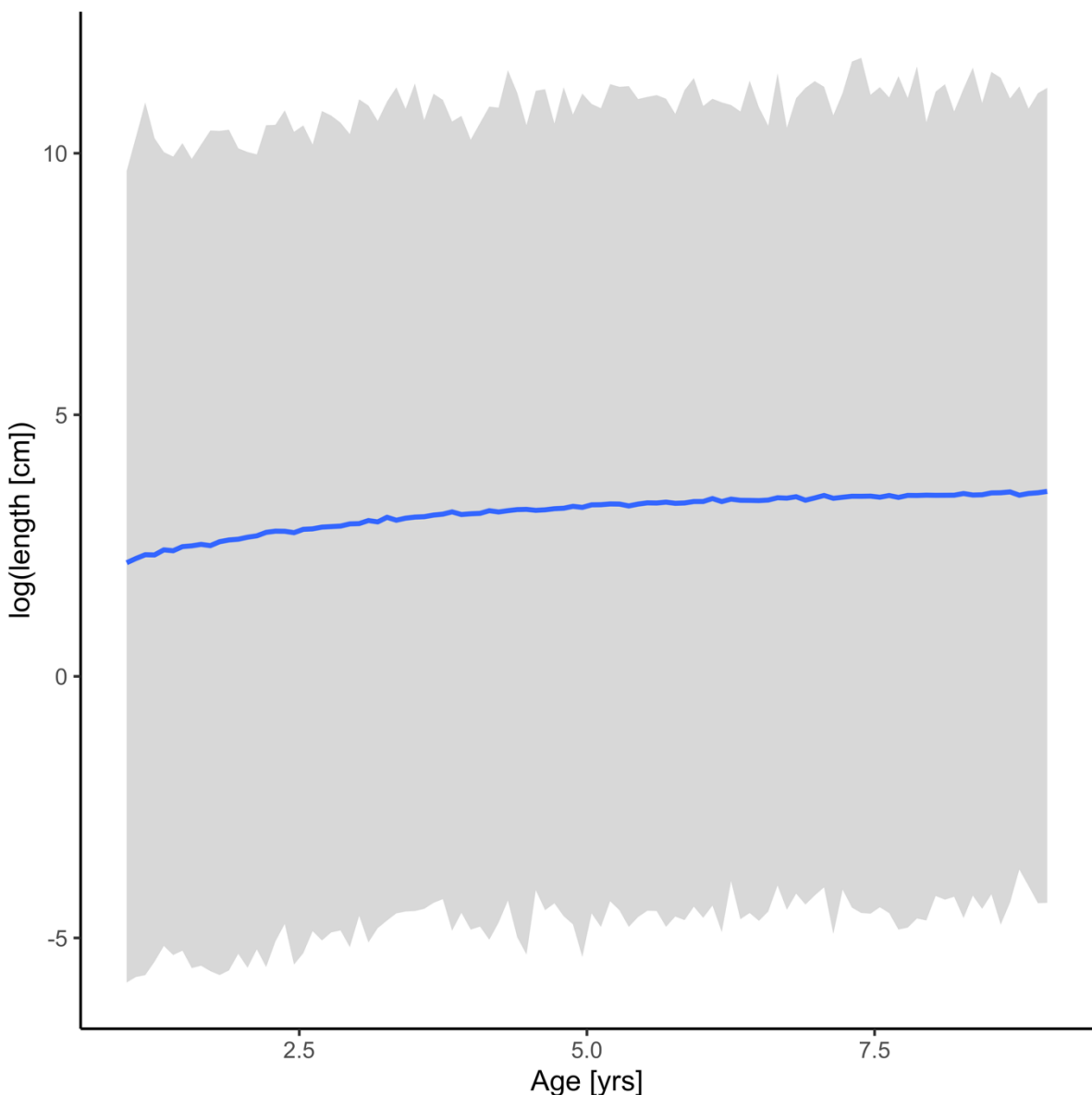
17

18

19

20

21



22

23 **Fig. S1.** Prior predictive distribution for the von Bertalanffy growth equation (posterior draws
24 from the prior only, ignoring the likelihood). The solid line is the median and the shaded area
25 is the 95% credible intervals.

26

27

28

29

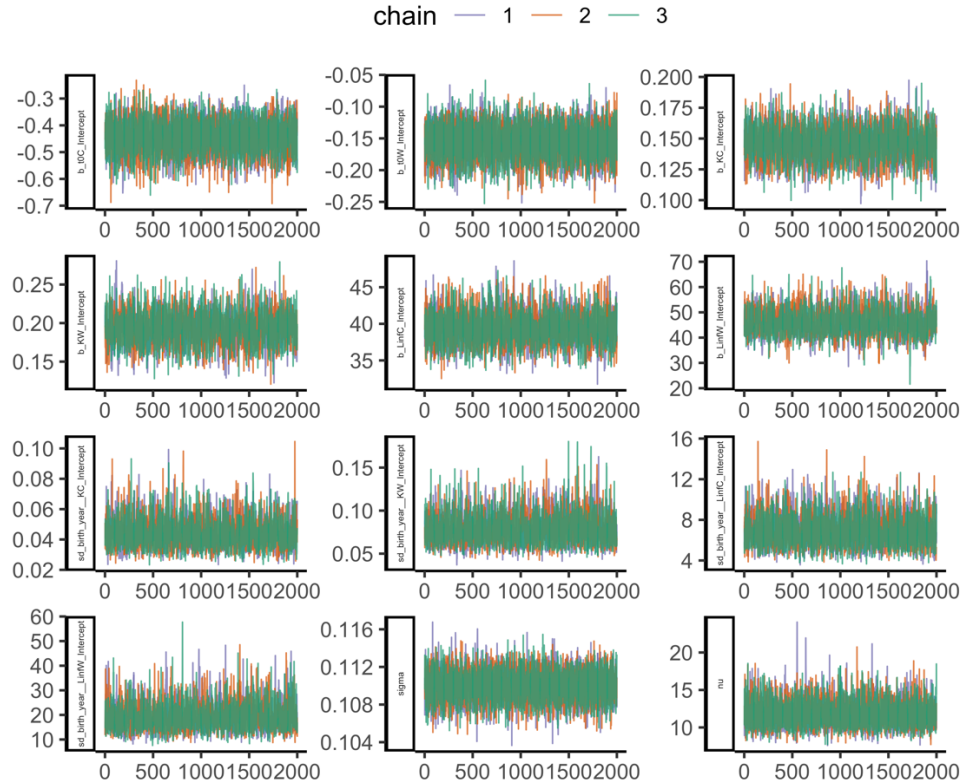
30

31 **Table S1.** Comparison of von Bertalanffy growth models with different combinations of
 32 shared and area-specific parameters (ordered by difference in expected log pointwise density
 33 (*elpd*) from the best model). Note that in all models, L_{∞_j} and K_j vary among cohorts.

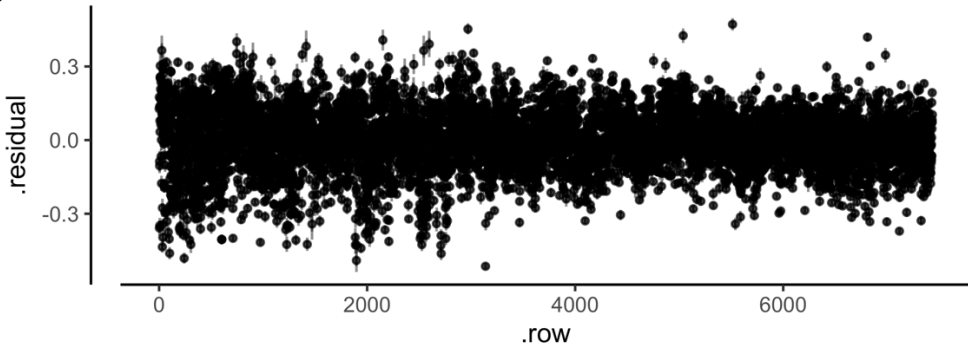
Model Name	Model structure	elpd_diff
M1	Area-specific L_{∞_j} , K_j and t_0	0
M4	Area-specific L_{∞_j} and K_j , common t_0	-9
M2	Area-specific K_j , common t_0 and L_{∞_j}	-111
M3	Area-specific t_0 and L_{∞_j} , common K_j	-150.5
M7	Area-specific L_{∞_j} , common K_j and t_0	-157.7
M6	Area-specific K_j , common t_0 and L_{∞_j}	-173.9
M5	Area-specific t_0 , common K_j and L_{∞_j}	-1337.5
M8	Common t_0 , K_j and L_{∞_j}	-2153.8

34
 35
 36
 37
 38
 39
 40
 41
 42
 43
 44

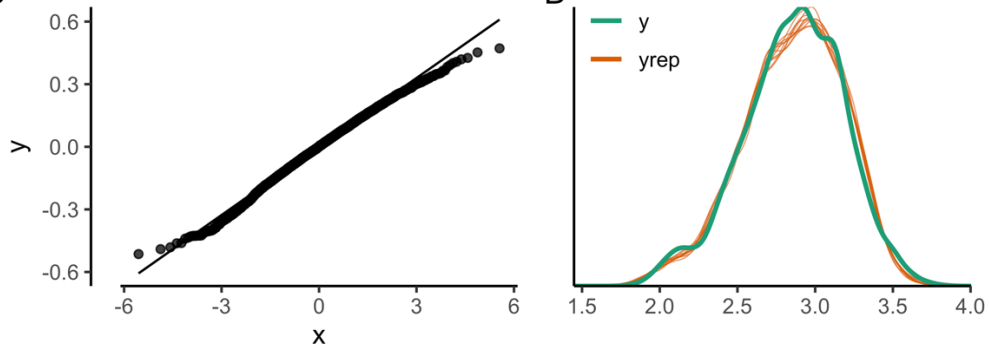
A



B

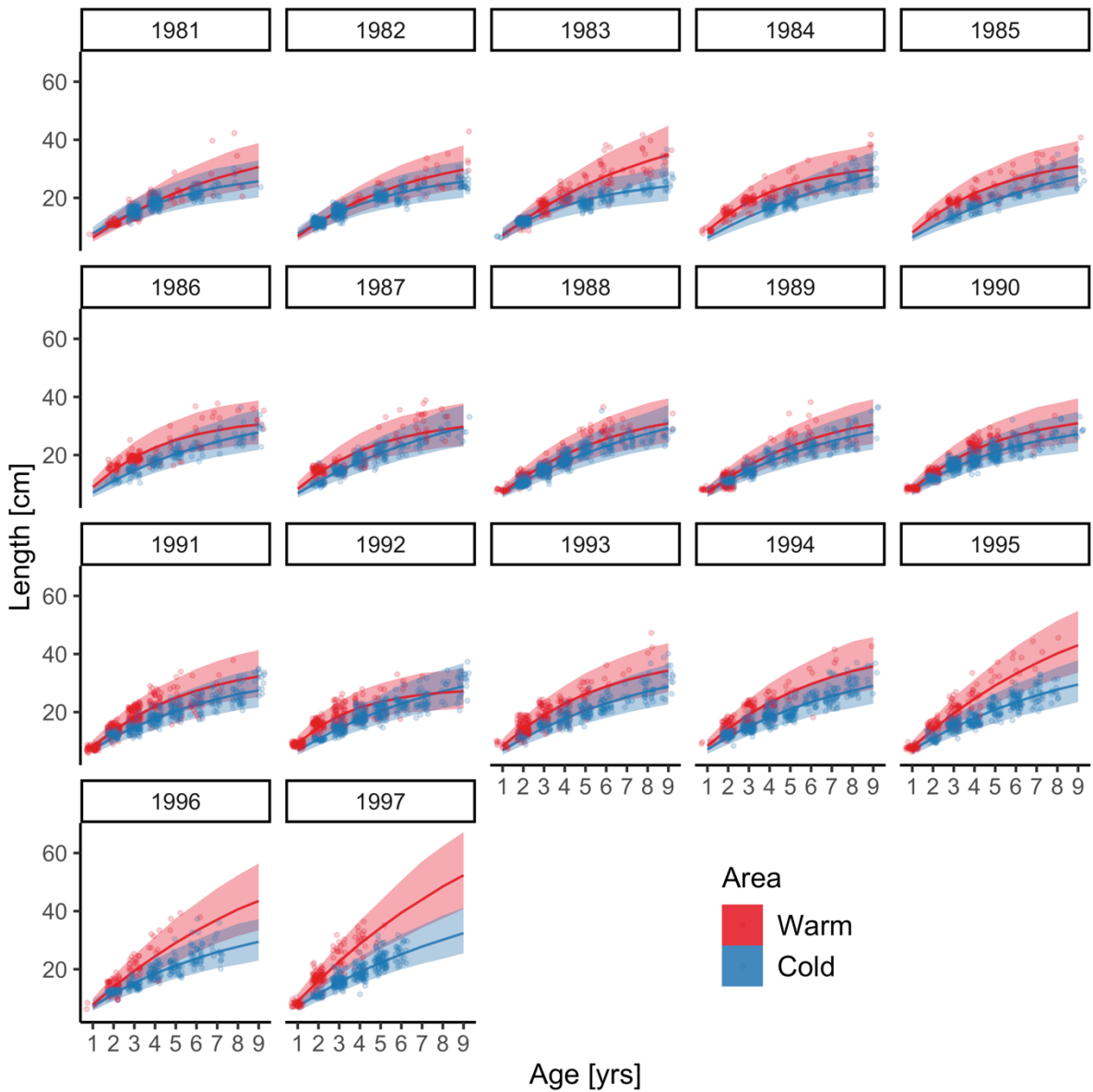


C



45

46 **Fig. S2.** The best model of the von Bertalanffy growth equation: (A) traceplot to illustrate chain
 47 convergence for key (population-level) parameters, (B) residuals, (C) QQ-plot and (D)
 48 posterior predictive check (D).



49

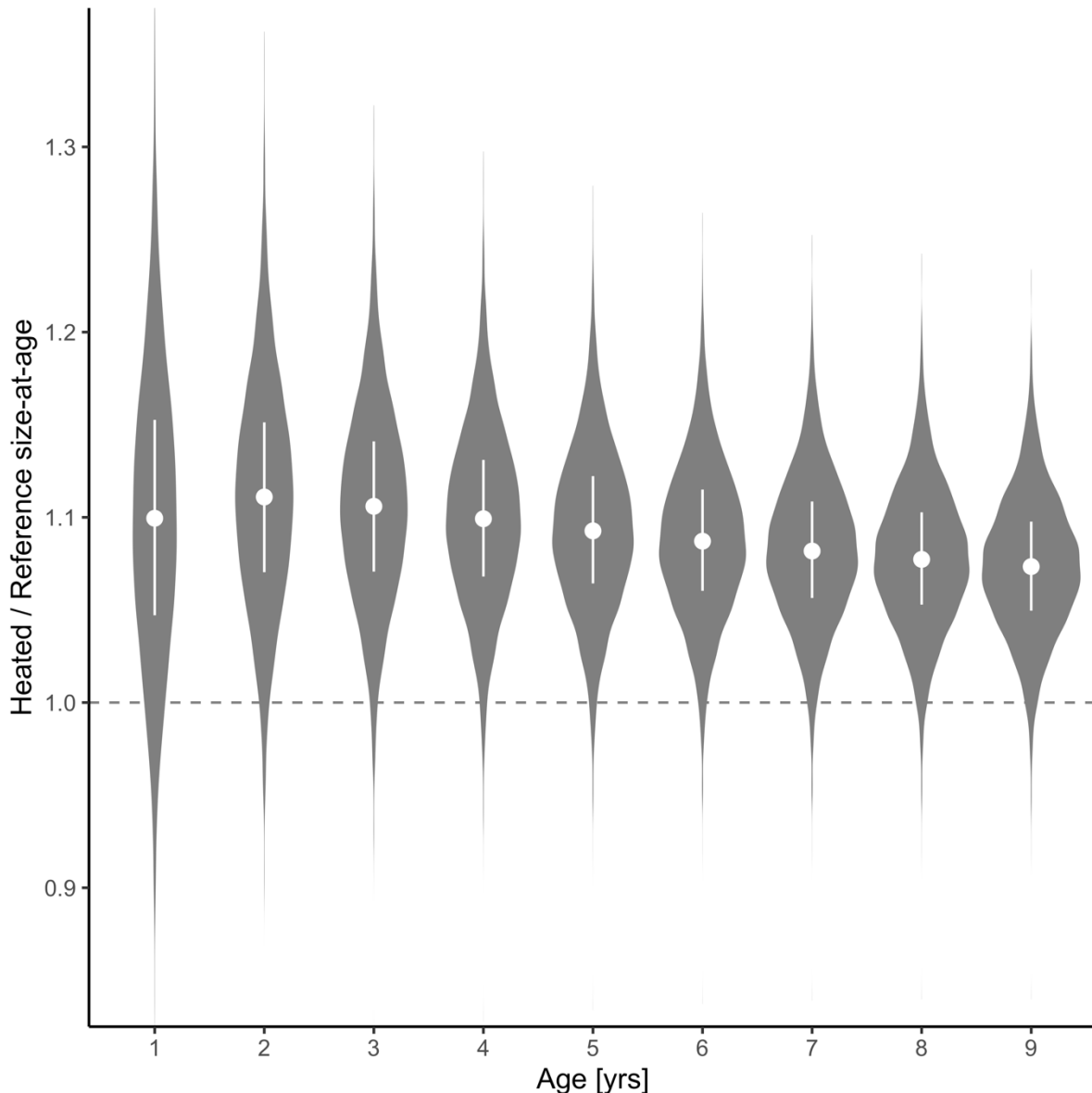
50 **Fig. S3.** Cohort-specific predictions from the best von Bertalanffy model (i.e., with cohort-
 51 varying L_∞ and K). Points correspond to data; solid lines correspond to the median of the
 52 posterior prediction from the model and the shaded area corresponds to the 95% credible
 53 interval.

54

55

56

57



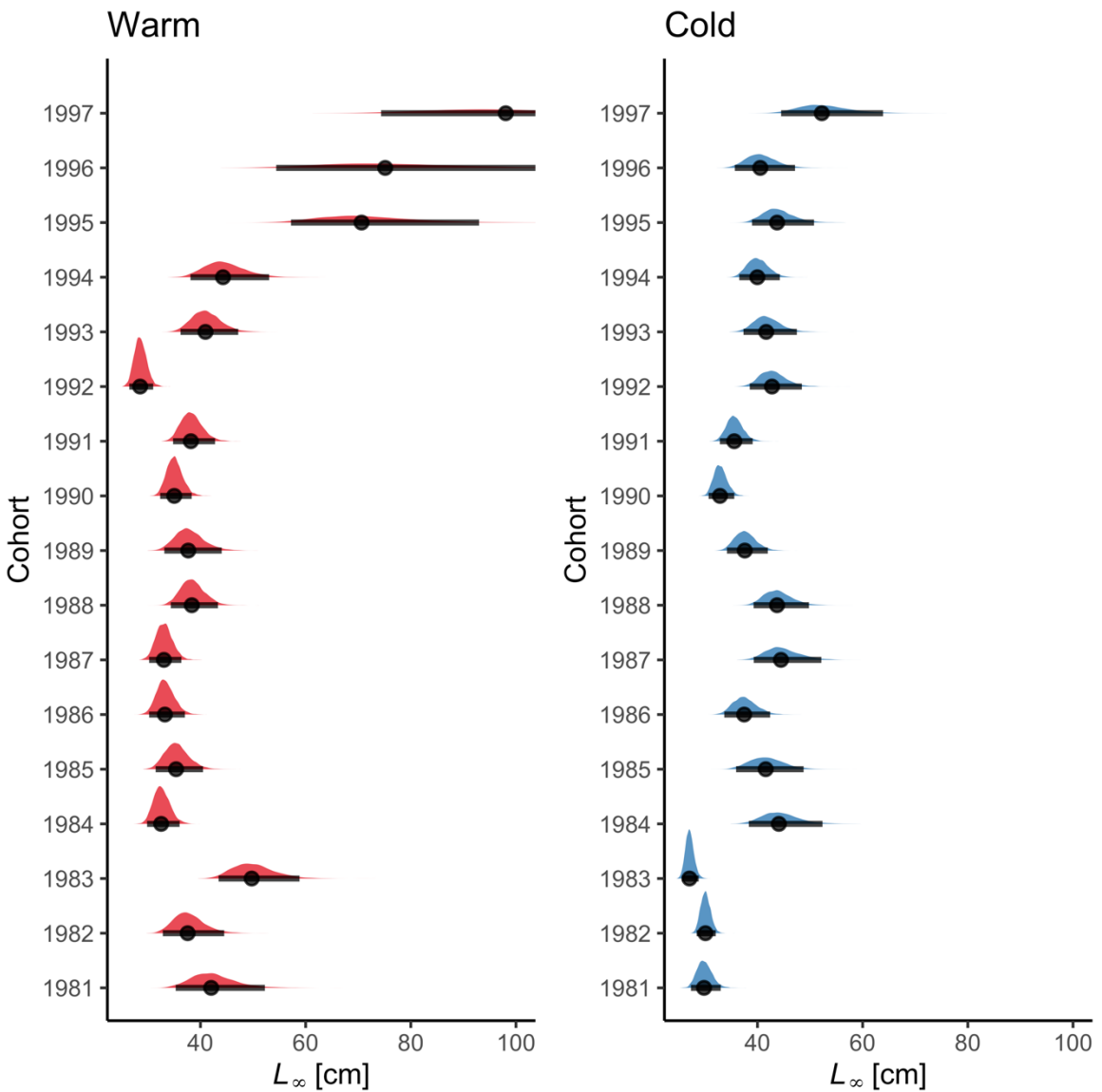
58

59 **Fig. S4.** The average length-at-age is larger for fish of all ages in the heated enclosed bay
 60 compared to the reference area, and the relative difference declines very slightly with age.
 61 Violin plots depict size-at-age in the heated relative to the reference area, based on draws from
 62 expectation of the posterior predictive distribution (without random effects). The points and
 63 vertical lines depict the median and the interquartile range.

64

65

66

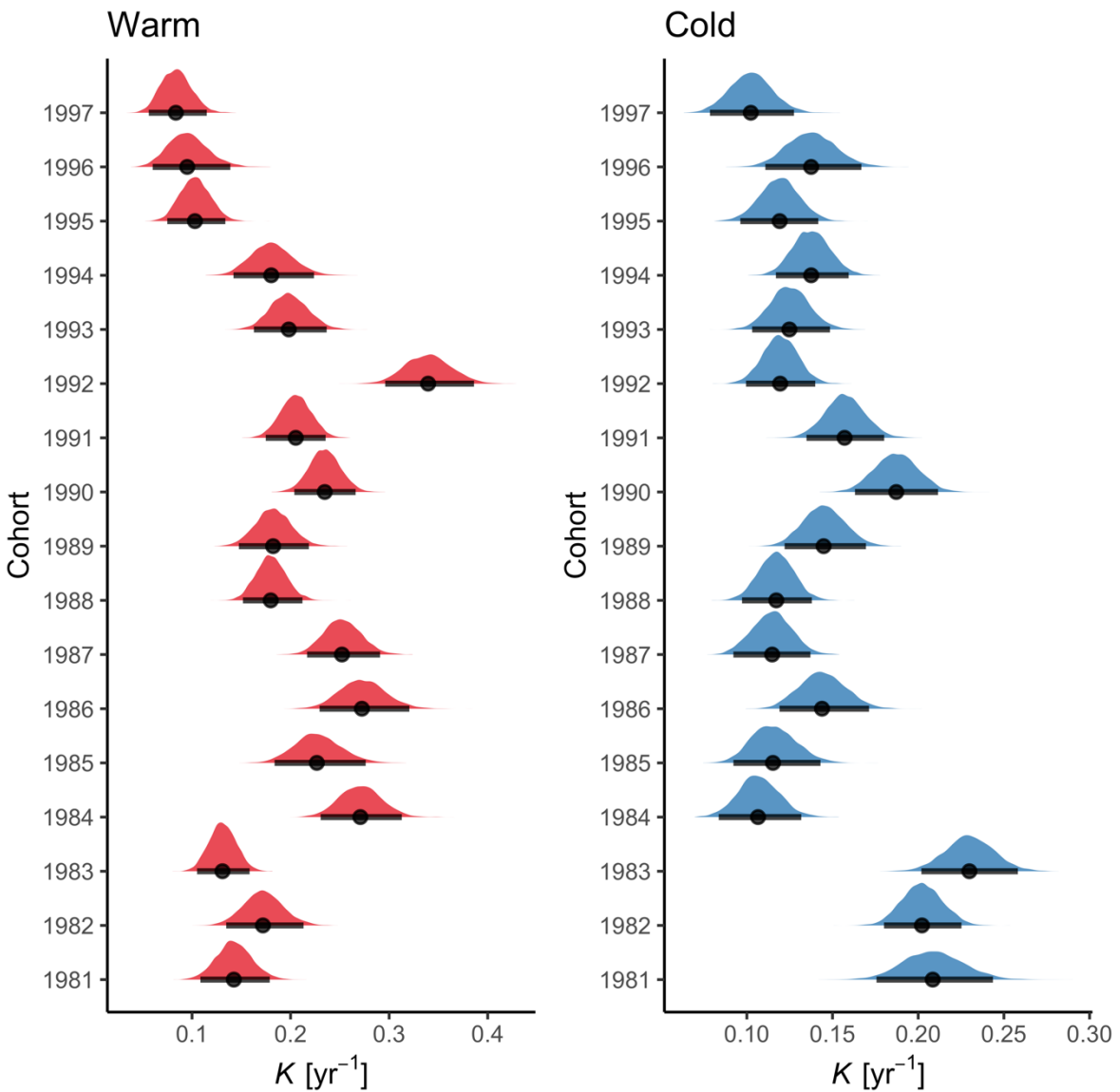


67

68 **Fig. S5.** Posterior distributions of the cohort-varying L_{∞} parameter in the best von Bertalanffy
 69 growth model. Points correspond to the median and the horizontal lines correspond to the 95%
 70 credible interval. Note that the distributions of L_{∞} in the warm areas extend beyond the x-axis
 71 for cohorts 1995–1997 (also evident in Fig. S3). The range of the x-axis was set to be wide
 72 enough to include the posterior medians of the larger estimates but narrow enough to allow for
 73 comparison between the other cohorts and areas.

74

75



76

77 **Fig. S6.** Posterior distributions of the cohort-varying K parameter in the von Bertalanffy model.

78 Points correspond to the median and the horizontal lines correspond to the 95% credible
79 interval.

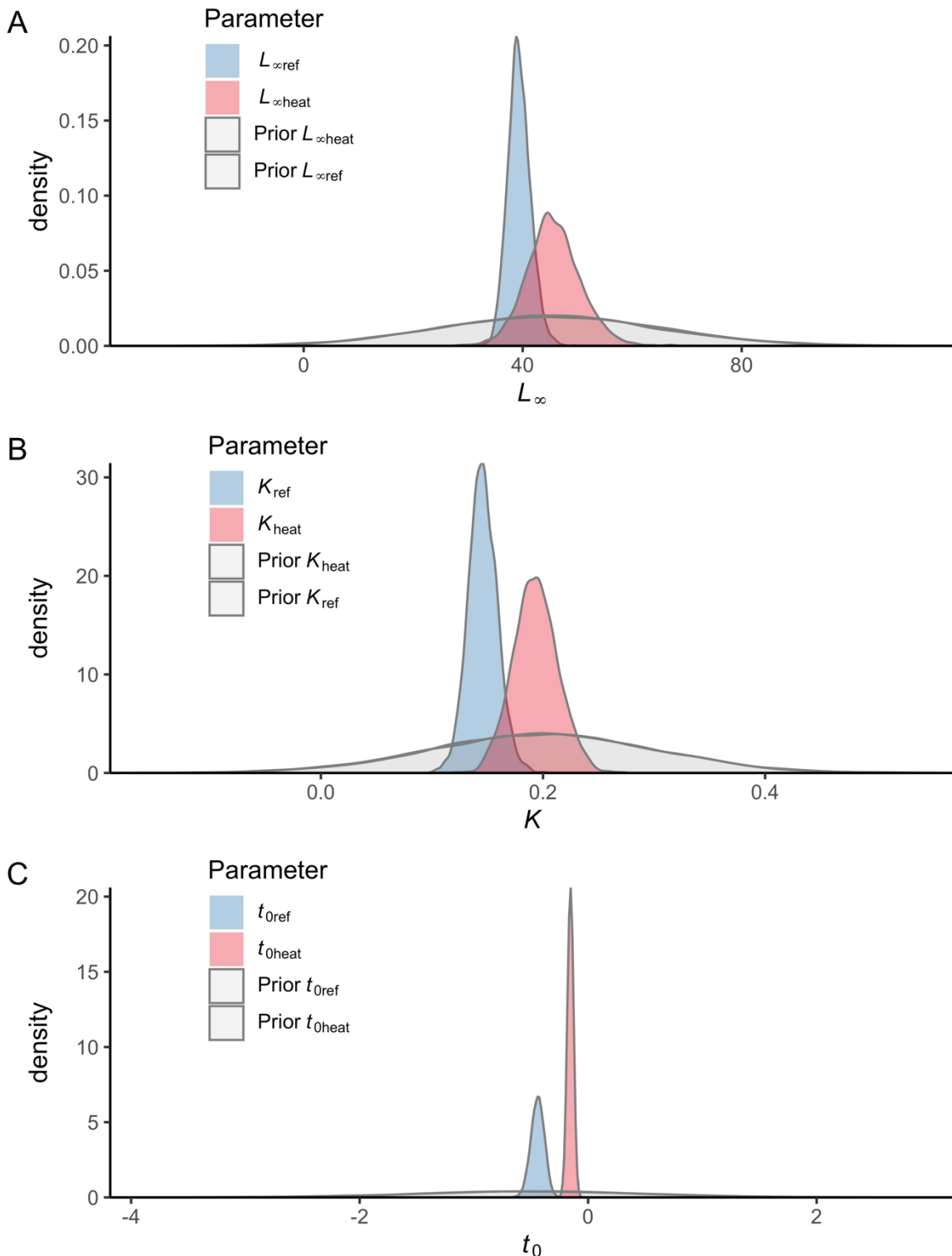
80

81

82

83

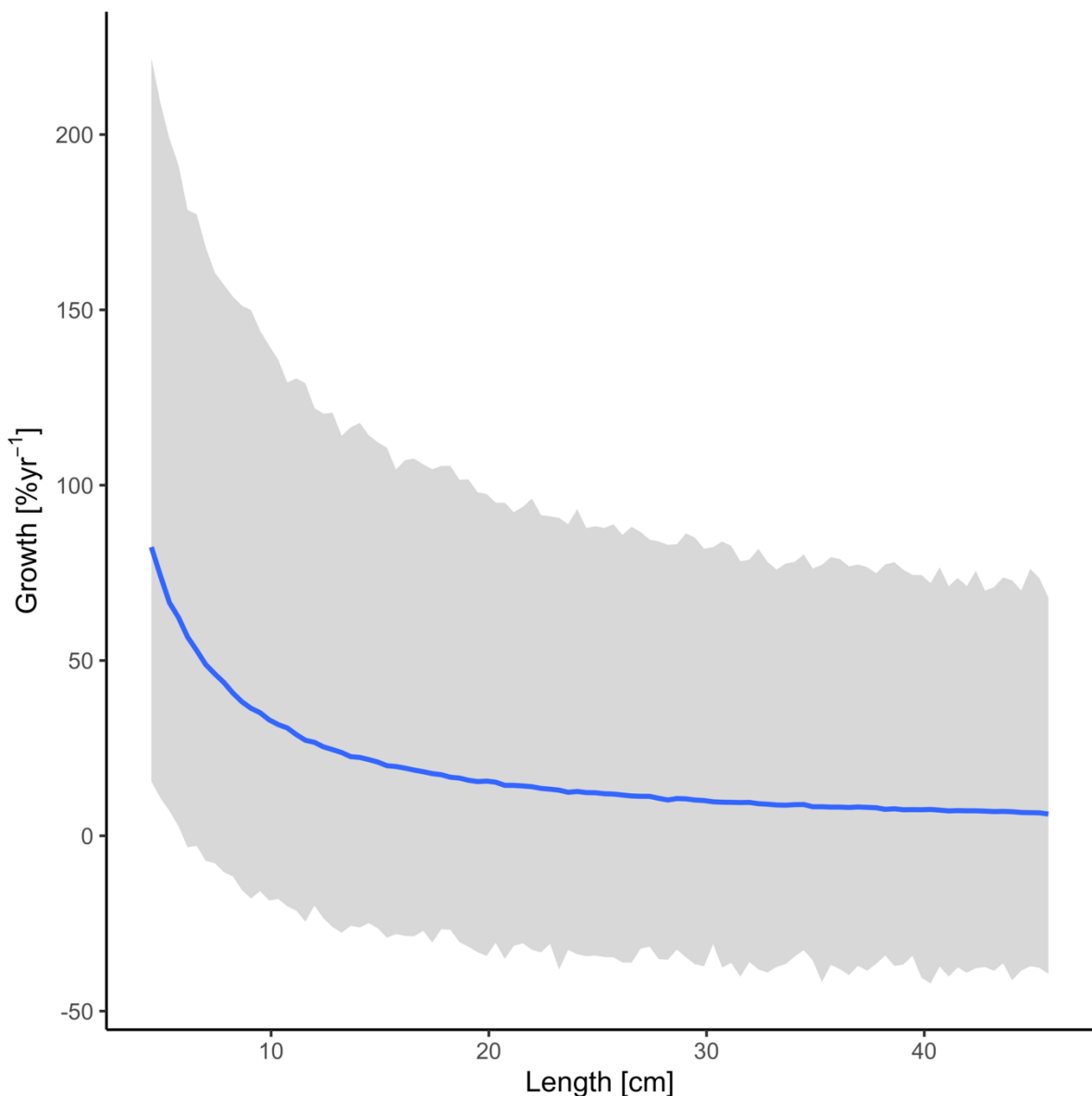
84



85

86 **Fig. S7.** Prior vs posterior distributions for parameters L_{∞} (A), K (B) and t_0 (C) in the best
87 model of the von Bertalanffy growth equation.

88



89

90 **Fig. S8.** Prior predictive distribution for the allometric growth model (posterior draws from the
91 prior only, ignoring the likelihood). The solid line is the median and the shaded area is the 95%
92 credible intervals.

93

94

95

96 **Table S2.** Comparison of allometric growth models with common or unique θ -parameter
97 (exponent in the allometric growth model), ordered by difference in expected log pointwise
98 density (elpd) from the best model.

Model Name	Model structure	elpd_diff
M1	Intercept ($\alpha_{j[i],k[i]}$) varying across individuals within cohorts, fixed, area-specific slope ($\theta_{\text{ref}}, \theta_{\text{heat}}$)	0
M2	Intercept ($\alpha_{j[i],k[i]}$) varying across individuals within cohorts, “fixed” common slope (θ)	-2.7

99

100

101

102

103

104

105

106

107

108

109

110

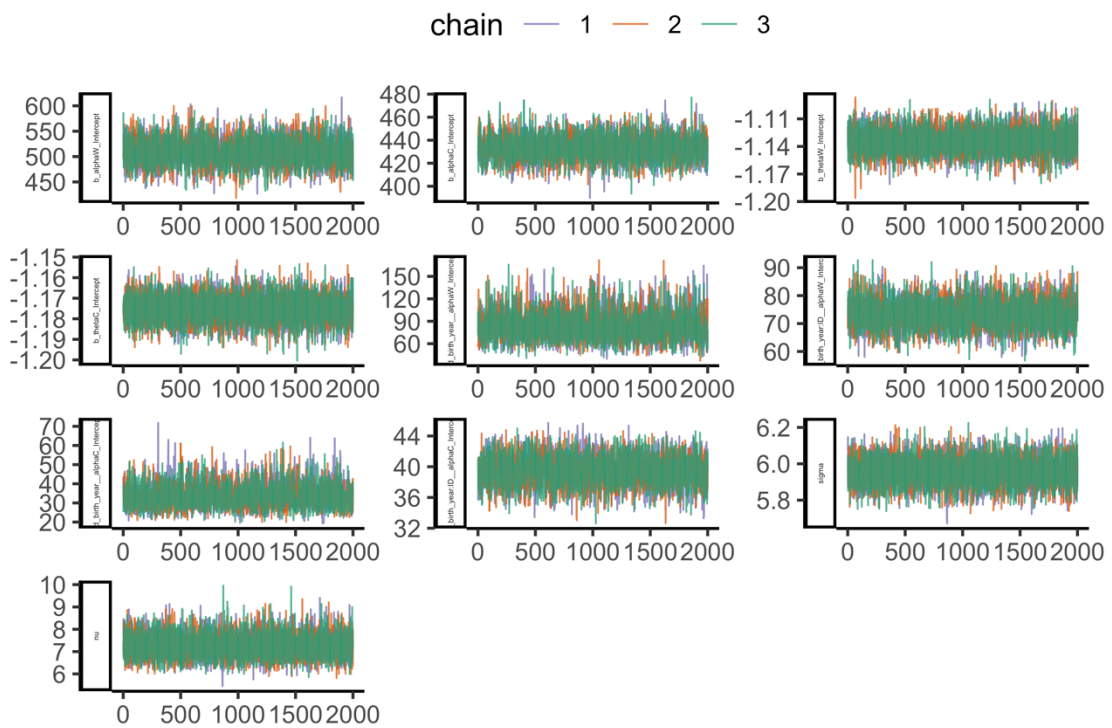
111

112

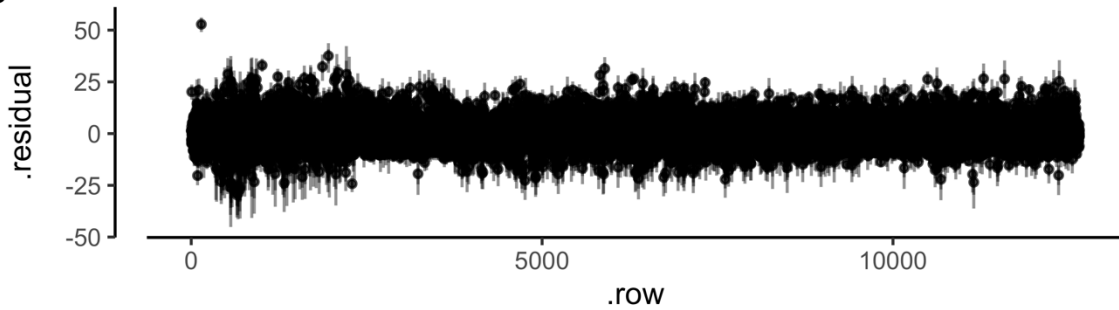
113

114

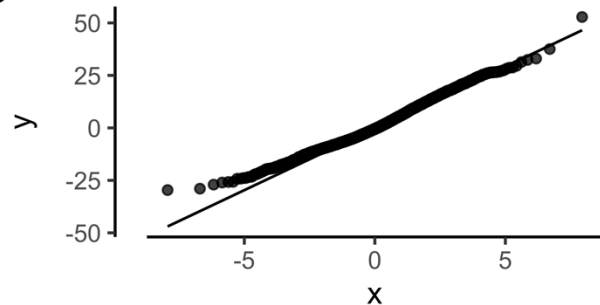
A



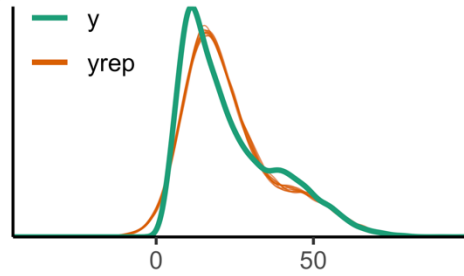
B



C



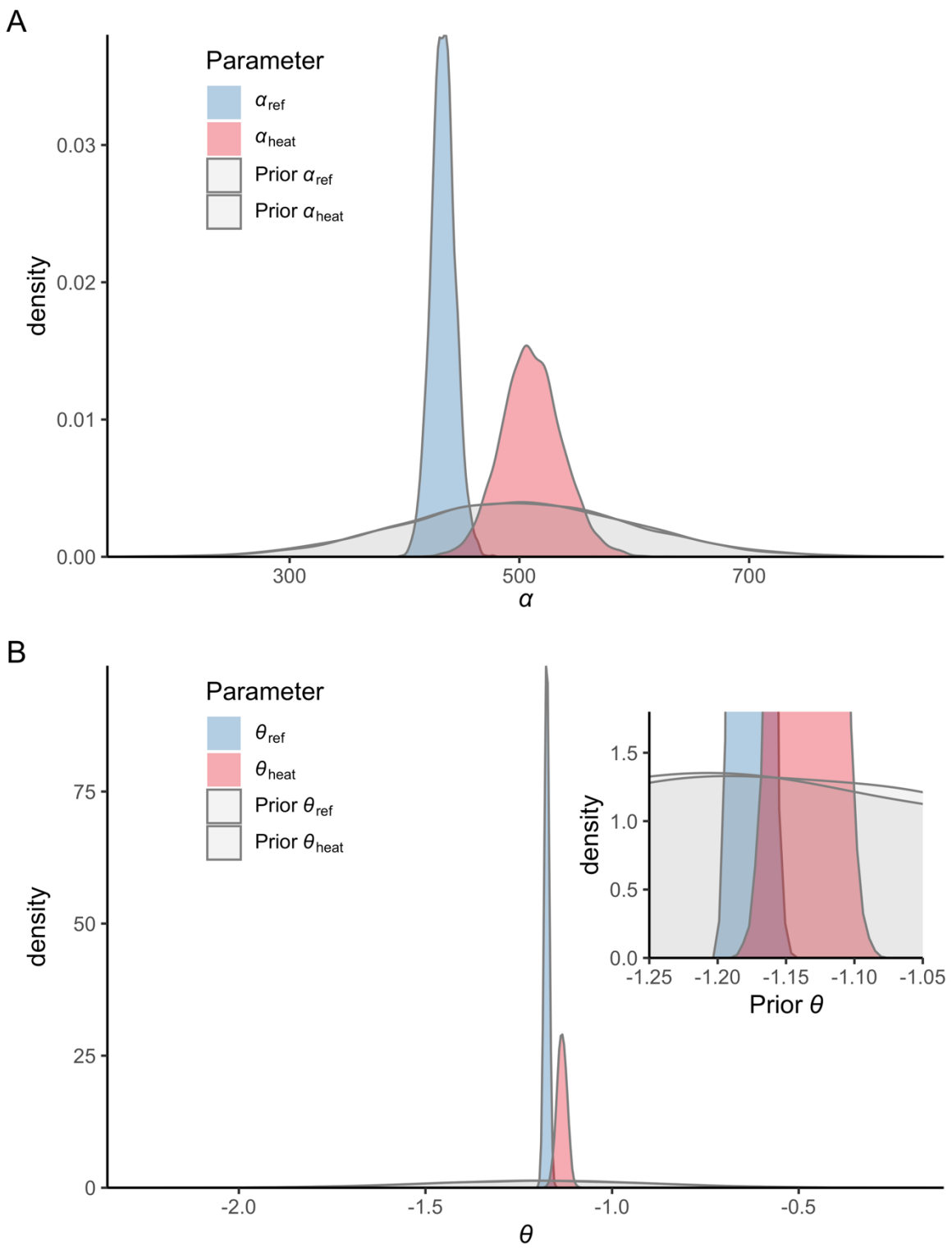
D



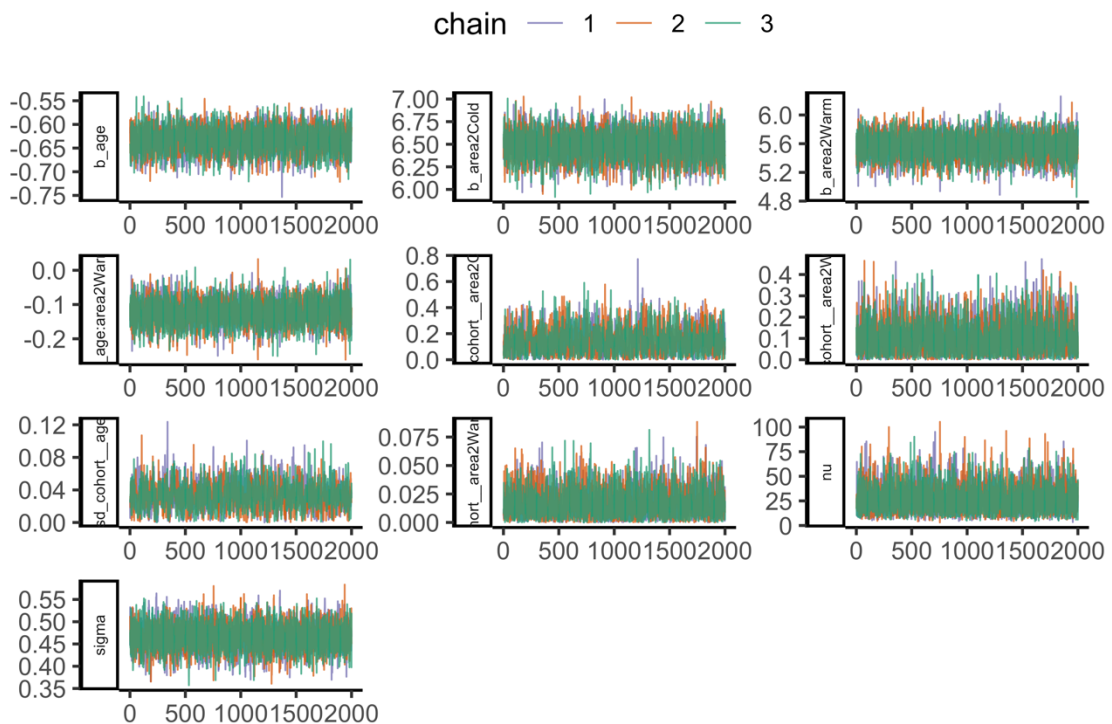
115

116 **Fig. S9.** The best allometric growth model: (A) traceplot to illustrate chain convergence for
 117 key (population-level) parameters, (B) residuals, (C) QQ-plot and (D) posterior predictive
 118 check (D).

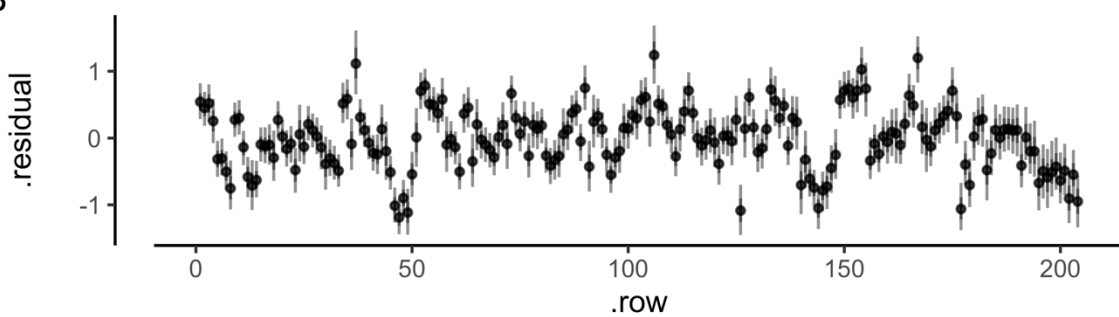
119



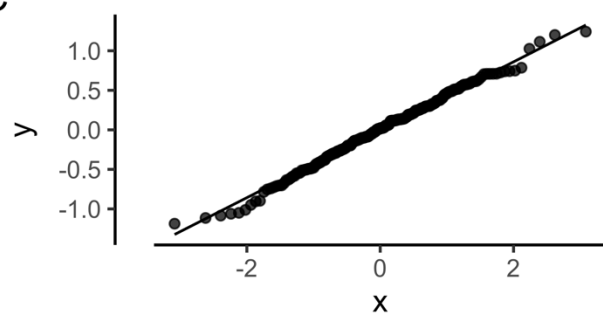
A



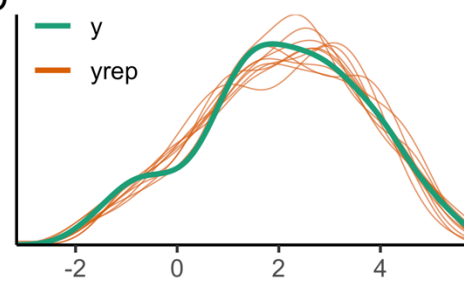
B



C



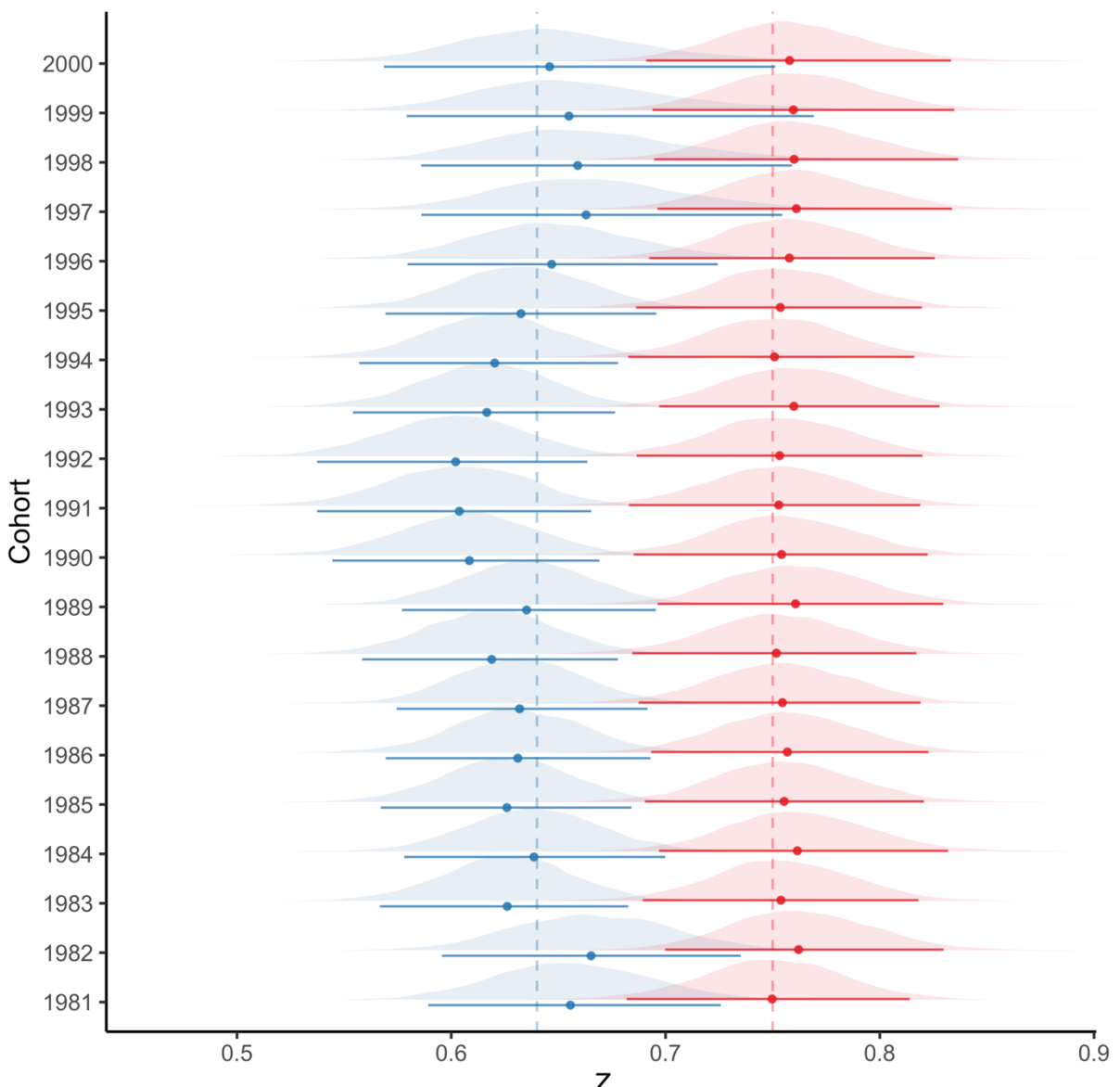
D



125

126 **Fig. S11.** The best catch curve model: (A) traceplot to illustrate chain convergence for key
 127 (population-level) parameters, (B) residuals, (C) QQ-plot and (D) posterior predictive check
 128 (D).

129



130

131 **Fig. S12.** Posterior distributions of the cohort-varying slopes in the best catch curve model,
 132 where Z , the mortality rate, is the negative of the slope of natural log of catch per unit effort
 133 (CPUE) as a function of age. Points correspond to the median and the vertical lines correspond
 134 to the 95% credible interval.

135

136

137

138

139